Proceedings of the 17th World Congress
The International Federation of Automatic Control
Seoul, Korea, July 6-11, 2008

Challenging the optimality of the pulse excitation in magnetic resonance imaging ⋆

B. Tahayori * L.A. Johnston * I.M.Y. Mareels * P.M. Farrell *

* *Department of Electrical and Electronic Engineering, and NICTA Victoria Research Laboratory The University of Melbourne, Australia (email: b.tahayori@ee.unimelb.edu.au)*

Abstract: The design of excitation signals for Magnetic Resonance Imaging (MRI) is cast as an optimal control problem. An appropriate cost criterion, the Signal Contrast Efficiency (SCE), is developed. It is to be optimised subject to dynamics expressed by the Bloch equation. The solution to the optimisation problem is potentially useful for all forms of MRI including structural and functional imaging. Here, we demonstrate that signals other than pulse excitations, which are ubiquitous in MRI, can provide adequate excitation, thus challenging the optimality and ubiquity of pulsed signals. A class of on-resonance piece-wise continuous amplitude modulated signals is introduced. It is shown that despite the bilinear nature of the Bloch equations, the optimisation problem is largely analytically tractable for this class of signals, using Galerkin approximation methods. Simulations demonstrate that this class of signals may provide an attractive alternative to pulsed excitation signals for MRI.

Keywords: Biomedical imaging systems, Magnetic resonance imaging, Optimal control, Bloch equation, Radio frequency excitation, Magnetisation, Contrast, Rabi frequency.

1. INTRODUCTION

Magnetic Resonance Imaging (MRI) is one of the major tomographic imaging modalities. A Magnetic Resonance (MR) signal is generated by recording the current induced in a receive coil by fluctuations in nuclear magnetisation produced by a time varying (Radio Frequency (RF)) externally applied magnetic field. The behaviour of the spin system at a classical level in the presence of an external field is completely described by the Bloch equation,

$$\dot{\mathbf{M}}(t) = \gamma \mathbf{M}(t) \times \mathbf{B}_{ext}(t) + \frac{1}{T_1}(M_0 - M_z(t))\mathbf{e}_z - \frac{1}{T_2}\mathbf{M}_{xy}(t). \tag{1}$$

Here, γ is the gyromagnetic ratio, and $\mathbf{e}_z$ is the unit vector in the z direction. T_1 and T_2 are longitudinal and transverse relaxation time constants, respectively. $\mathbf{M}$ is the bulk magnetisation vector (to be measured), dependent on both position and time. $M_0\mathbf{e}_z$ is the thermal equilibrium created by an ideally-uniform static field oriented in the z-direction (aligned with the static external field).

In the above equation the external field is the superposition of a static and uniform magnetic field in the z-direction (with amplitude B_0), and a time varying, spatially dependent, excitation field, $\mathbf{B}_{xy}(t)$, expressed as

$$\mathbf{B}_{ext}(t) = \mathbf{B}_{xy}(t) + B_0\mathbf{e}_z. \tag{2}$$

In order to identify and spatially localise the MR signal from the induced current, which is a function only of time, gradient fields are carefully designed to map spatial dependency to frequency dependency in the received signal, a property that is enabled by the fact that proton spin frequency at a particular location scales linearly with the magnitude of the external field at that location.

The first step in two dimensional MR imaging is typically to excite a thin slice of the object by applying a selective RF pulsed magnetic field. To reduce partial volume effects, the design of a RF pulse with good frequency selectivity is of crucial importance. Slice selection is based on the Bloch equation, which is nonlinear in nature.

From the early days of MRI, several methods have been proposed to solve the selective excitation problem [Garroway et al., 1974]. These methods have been derived through approximate solutions to the Bloch equation [Conolly and Macovski, 1985], or are based on computer simulations that predict the magnetisation response of the spin system to various excitatory inputs [Loeffler et al., 1983]. For small flip angles (the amount of perturbation of the local thermal equilibrium magnetisation from its initial orientation), the design of the selective pulse is based on the Fourier analysis of the Bloch equation [Hinshaw and Lent, 1983], valid for flip angles smaller than $\pi/2$. The design of better pulses requires application of optimal control theory [Pauly et al., 1991, Conolly et al., 1996, Brockett and Khaneja, 2001, Ulloa et al., 2004].

Conolly et al. [1996] provide a mathematical basis for RF pulse design and an algorithm to solve for the optimal pulse, defined to be the pulse that steers the magnetisation from the initial state closest to the desired final state. It is shown that such an optimal control does exist.

The Shinner-Le Roux method is a recursive algorithm for finding the optimal pulse for selective excitation [Pauly

⋆ This work is supported by NICTA Lifesciences, the Victorian Research Laboratory.

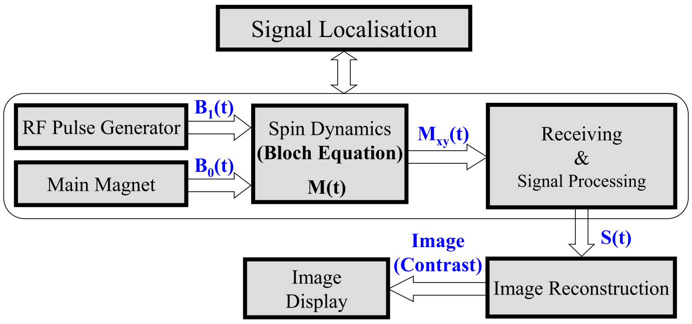

Fig. 1. A general block diagram of the MRI system.

et al., 1991]. This method is based on a discrete approximation to the Bloch equation which simplifies the solution of the selective pulse to the design of two polynomials.

Brockett and Khaneja [2001] consider stochastic models for constructing the optimal excitation, based on a conditional entropy approach. In practice, due to field inhomogeneities, application of an on-resonance pulse cannot simultaneously excite an ensemble of spins. Li and Khaneja [2006] have formulated and solved this problem, finding a procedure to design compensating pulses that are able to simultaneously bring all the desired spins into the transverse plane.

Improvements to the received MR signal may be achieved via two principal approaches. First, it is possible to increase the received signal strength through better hardware design, including higher strength magnetic fields, more homogeneous fields, and more sensitive coils. The second approach is via design of a more efficient RF excitation signal. In this paper we focus on the latter method. We formulate the image contrast optimisation problem based on the Bloch equation, and demonstrate the feasibility of maintaining spin coherency for a novel continuous wave excitation signal, thus providing a potential alternative to the traditional pulsed MR excitation.

2. PROBLEM STATEMENT

A block diagram of the MRI system is depicted in Figure 1. The inputs to this system are the main static field and the RF excitation signal. The result of the RF excitation is an MR signal that, if encoded properly, retains spatial information about the object. No rigorous mathematical analyses exist in the MRI literature proving optimality of pulse excitation for generation of image contrast. We therefore formulate the optimisation problem in order to determine whether pulses, or some other form of excitation signal, generate the optimal contrast between tissue types in the resultant images.

2.1 Problem Formulation

In the laboratory frame of reference, the Bloch equation in the presence of the static, gradient and excitation fields is written as

$$\begin{bmatrix} \dot{M}_x \\ \dot{M}_y \\ \dot{M}_z \end{bmatrix} = \begin{bmatrix} -\dfrac{1}{T_2} & \gamma B_z(t) & \gamma B_y(t) \\ -\gamma B_z(t) & -\dfrac{1}{T_2} & \gamma B_x(t) \\ -\gamma B_y(t) & -\gamma B_x(t) & -\dfrac{1}{T_1} \end{bmatrix} \begin{bmatrix} M_x \\ M_y \\ M_z \end{bmatrix} + \begin{bmatrix} 0 \\ 0 \\ \dfrac{M_0}{T_1} \end{bmatrix}, \tag{3}$$

in which the field in the z direction is given by

$$B_z = B_0 + \Delta B_0(t) + \mathbf{G_r}(t) \cdot \mathbf{r}, \tag{4}$$

where $\Delta B_0(t)$ represents field inhomogeneities, $\mathbf{G_r}(t)$ is the gradient field, and $\mathbf{r}$ is position.

If B_0, and consequently B_z, are permitted to change considerably with time, then since both T_1 and T_2 are functions of the field strength [Alster and Burdette, 2001], the relaxation time constants become time dependent as well. Thus, in the more general case, the Bloch equation may be written as

$$\begin{bmatrix} \dot{M}_x \\ \dot{M}_y \\ \dot{M}_z \end{bmatrix} = \begin{bmatrix} -\dfrac{1}{T_2(t)} & \omega_z(t) & \omega_y(t) \\ -\omega_z(t) & -\dfrac{1}{T_2(t)} & \omega_x(t) \\ -\omega_y(t) & -\omega_x(t) & -\dfrac{1}{T_1(t)} \end{bmatrix} \begin{bmatrix} M_x \\ M_y \\ M_z \end{bmatrix} + \begin{bmatrix} 0 \\ 0 \\ \dfrac{M_0(t)}{T_1(t)} \end{bmatrix} \tag{5}$$

where the frequency terms are given by the Larmor relationship,

$$\omega_i(t) = \gamma B_i(t), \qquad i = x, y, z. \tag{6}$$

In particular, $\omega_z = \gamma B_z$ is referred to as the Larmor frequency. The excitation field can be expressed as

$$\mathbf{B}_{xy}(t) \;\equiv\; \mathbf{B}_1(t) \;=\; \frac{1}{\gamma}\Big(u(t)\,\mathbf{e}_x + v(t)\,\mathbf{e}_y\Big), \tag{7}$$

where

$$u(t) \;=\; \gamma B_x^e(t)\cos\big(\omega_{rf}(t)\,t + \phi_x(t)\big) \tag{8a}$$
$$v(t) \;=\; -\gamma B_y^e(t)\sin\big(\omega_{rf}(t)\,t + \phi_y(t)\big). \tag{8b}$$

We consider $\mathbf{u}(t) = [u(t), v(t)]^T$, for $u, v \in \mathcal{U}$, where $\mathcal{U}$ is the set of all admissible piecewise continuous bounded functions. By appropriate selection of the parameters in (8) it is possible to generate any desirable piecewise continuous function.

After transformation of the Bloch equation to the frame rotating at $\omega_{rf}(t)$, represented by the axes $\{x', y', z'\}$ so as to distinguish it from the laboratory frame of reference [Tahayori et al., 2007], we obtain

$$\begin{bmatrix} \dot{M}_{x'} \\ \dot{M}_{y'} \\ \dot{M}_{z'} \end{bmatrix} = \mathbf{\Omega}'\Big(\mathbf{u}(t), \mathbf{B}_z(t)\Big) \begin{bmatrix} M_{x'} \\ M_{y'} \\ M_{z'} \end{bmatrix} + \begin{bmatrix} 0 \\ 0 \\ \dfrac{M_0(t)}{T_1(t)} \end{bmatrix}, \tag{9}$$

where

$$\mathbf{\Omega}'\Big(\mathbf{u}(t), \mathbf{B}_z(t)\Big) = \begin{bmatrix} -\dfrac{1}{T_2(t)} & \Delta\omega(t) & v_{tr}(t) \\ -\Delta\omega(t) & -\dfrac{1}{T_2(t)} & u_{tr}(t) \\ -v_{tr}(t) & -u_{tr}(t) & -\dfrac{1}{T_1(t)} \end{bmatrix}, \tag{10}$$

in which

$$u_{tr}(t) = u(t)\cos\big(\omega_{rf}(t)\,t\big) + v(t)\sin\big(\omega_{rf}(t)\,t\big), \tag{11a}$$
$$v_{tr}(t) = -u(t)\sin\big(\omega_{rf}(t)\,t\big) + v(t)\cos\big(\omega_{rf}(t)\,t\big), \tag{11b}$$
$$\Delta\omega(t) = \Delta\omega_{rf}(\mathbf{r}, t) + \delta\omega(t). \tag{11c}$$

Here $\Delta\omega_{rf}(\mathbf{r}, t)$ represents the difference between the instantaneous Larmor frequency of the main magnet with superimposed gradients, and the instantaneous rotation frequency of the RF field

$$\Delta\omega_{rf}(\mathbf{r},t) = \gamma\big(B_0(t) + \mathbf{G_r}(t)\cdot\mathbf{r}\big) - \omega_{rf}(t). \tag{12}$$

Since we may have control over both the static field and the RF field, $\Delta\omega_{rf}(\mathbf{r},t)$ can be considered a free parameter. $\delta\omega(t)$ represents all field inhomogeneities other than those comprising $\Delta\omega_{rf}(\mathbf{r},t)$. These inhomogeneities include any imperfections in the main magnet, chemical shifts, knight shifts, and paramagnetic shift effects [Levitt, 2001]. Thus $\delta\omega(t) = \gamma\,\Delta B_0(t)$ represents all the stochastic fluctuations in the spin system.

For two different tissue types, a and b, with the following spin properties

$$\boldsymbol{\theta}_a(t) = \begin{bmatrix} T_{1a}(t) \\ T_{2a}(t) \\ M_{0a}(t) \end{bmatrix}, \qquad \boldsymbol{\theta}_b(t) = \begin{bmatrix} T_{1b}(t) \\ T_{2b}(t) \\ M_{0b}(t) \end{bmatrix}, \tag{13}$$

the system parameters in (9) are tissue dependent,

$$\boldsymbol{\Omega'}_i\Big(\boldsymbol{\theta}_i, \mathbf{u}(t), \mathbf{B}_z(t)\Big) = \begin{bmatrix} -\dfrac{1}{T_{2i}(t)} & \Delta\omega_i(t) & v_{tr}(t) \\ -\Delta\omega_i(t) & -\dfrac{1}{T_{2i}(t)} & u_{tr}(t) \\ -v_{tr}(t) & -u_{tr}(t) & -\dfrac{1}{T_{1i}(t)} \end{bmatrix}, \tag{14}$$

$$\Delta\omega_i(t) = \Delta\omega_{rf}(\mathbf{r},t) + \delta\omega_i(t), \quad i = a,b, \tag{15}$$

resulting in the Bloch equation dynamics,

$$\dot{\mathbf{M}}'_a(t) = \boldsymbol{\Omega}'_a\Big(\boldsymbol{\theta}_a, \mathbf{u}(t), \mathbf{B}_z(t)\Big)\mathbf{M}'_a(t) + \frac{\mathbf{M}_{0a}(t)}{T_{1a}(t)}, \tag{16a}$$

$$\dot{\mathbf{M}}'_b(t) = \boldsymbol{\Omega}'_b\Big(\boldsymbol{\theta}_b, \mathbf{u}(t), \mathbf{B}_z(t)\Big)\mathbf{M}'_b(t) + \frac{\mathbf{M}_{0b}(t)}{T_{1b}(t)}, \tag{16b}$$

with the following initial conditions

$$\mathbf{M}'_a(0) = \begin{bmatrix} 0 \\ 0 \\ M_{0a}(0) \end{bmatrix}, \quad \mathbf{M}'_b(0) = \begin{bmatrix} 0 \\ 0 \\ M_{0b}(0) \end{bmatrix}. \tag{17}$$

Since the induced voltage created by the transverse magnetisation generates the MR signal, the intensity of the final image is proportional to the magnetisation in the $x'y'$ plane. A scaling factor takes into account the coil sensitivity and image reconstruction technique. The signal intensity may therefore be expressed as

$$\text{Signal Intensity} \propto \int_0^T \Big|\mathbf{M}_{x'y'}(t)\Big|\, dt. \tag{18}$$

The overall objective is to maximise the contrast to noise ratio of the final image. It is reasonable to assume that the noise distribution for imaging a given object is approximately constant across different types of excitation [Haacke et al., 1999]. The imaging procedure should be completed in the shortest possible time, so as to minimise exposure to the magnetic fields. We therefore define a performance measure similar to the imaging efficiency parameter [Haacke et al., 1999], and denote it by Signal Contrast Efficiency (SCE). SCE is defined to be the time normalised difference in signal from the two tissues, integrated over time

$$\text{Signal Contrast Efficiency} = \mathcal{J}\big(\boldsymbol{\theta}_a, \boldsymbol{\theta}_b, \mathbf{u}, \mathbf{B}_z\big) \triangleq \frac{\int_0^T \big|\mathbf{M}_{x'y'_a}(\boldsymbol{\theta}_a, \mathbf{u}(t), \mathbf{B}_z(t), t) - \mathbf{M}_{x'y'_b}(\boldsymbol{\theta}_b, \mathbf{u}(t), \mathbf{B}_z(t), t)\big|dt}{\sqrt{T}} \tag{19}$$

where T represents the duration of the excitation. As a result, for two different tissues' spin systems described by (16), we seek the optimal excitation waveform, $\mathbf{u}^*$, such that

$$\mathbf{u}^* = \underset{\mathbf{u}}{\operatorname{argmax}}\ \mathcal{J}\big(\boldsymbol{\theta}_a, \boldsymbol{\theta}_b, \mathbf{u}, \mathbf{B}_z\big) \tag{20}$$

while constraining the Specific Absorption Rate (SAR) to be less than a predefined threshold,

$$\int_0^T \sqrt{u(t)^2 + v(t)^2}\, dt \ \le\ A_{max} \tag{21}$$

The quantity, A_{max}, depends on the strength of the main magnet and properties of the object.

Theoretically, it is possible to have full control over the free parameters of the system, $\mathbf{u}$, $\Delta\omega_{rf}(t)$, and $\mathbf{B}_z$. We will allow B_z to change according to a predefined pattern. The parameters, T_1 and T_2, are known to change with $B_z(t)$ and we may have some control over them, however they are not free parameters of the system.

If instead we wish to determine the maximum contrast during a fixed period of time, then the objective function reduces to finding $\mathbf{u}^*$ such that

$$\mathbf{u}^* = \underset{\mathbf{u}}{\operatorname{argmax}} \int_0^T \Big|\mathbf{M}_{x'y'_a}(\boldsymbol{\theta}_a, \mathbf{u}(t), \mathbf{B}_z(t), t) - \mathbf{M}_{x'y'_b}(\boldsymbol{\theta}_b, \mathbf{u}(t), \mathbf{B}_z(t), t)\Big|\, dt \tag{22}$$

To maximise the image intensity, the signal intensity for one type of tissue must be maximised. Thus in this case the objective is to find a control such that

$$\mathbf{u}^* = \underset{\mathbf{u}}{\operatorname{argmax}} \frac{\int_0^T \Big|\mathbf{M}_{x'y'_a}\big(\boldsymbol{\theta}_a, \mathbf{u}(t), \mathbf{B}_z(t), t\big)\Big|dt}{\sqrt{T}}. \tag{23}$$

2.2 Problem Simplification

The spin systems for two tissue types written in their most general form, as in (16), evolve according to sets of time-varying parameters. The resultant optimisation problem is therefore very difficult to solve in this most general case. For simplification of the problem, we assume that B_z, and as a result T_{1i}, and T_{2i}, do not vary with time. Furthermore, we assume that the excitation is applied on-resonance, $\omega_{rf}(\mathbf{r},t) = \gamma\big(B_0(t) + \mathbf{G_r}(t)\cdot\mathbf{r}\big)$, and $B_x^e(t) = B_y^e(t) = B_1^e(t)$, $\phi_x(t) = \phi_y(t) = 0$ for all t and time-independent field inhomogeneities, resulting in

$$\dot{\mathbf{M}}'_i(t) = \Big(\mathbf{A}_i + \gamma B_1^e(t)\mathbf{B}\Big)\mathbf{M}'_i(t) + \frac{\mathbf{M}_{0i}}{T_{1i}}, \qquad i = a,b, \tag{24}$$

where

$$\mathbf{A}_i = \begin{bmatrix} -\frac{1}{T_{2i}} & \delta\omega & 0 \\ -\delta\omega & -\frac{1}{T_{2i}} & 0 \\ 0 & 0 & -\frac{1}{T_{1i}} \end{bmatrix}, \quad \mathbf{B} = \begin{bmatrix} 0 & 0 & 0 \\ 0 & 0 & 1 \\ 0 & -1 & 0 \end{bmatrix}. \tag{25}$$

The objective is to find the control $B_1^e(t)$ that maximises the Signal Contrast Efficiency, as defined in (19).

3. SIMULATION RESULTS

Most excitation waveforms, when applied for a long period of time, will cause the spins to dephase, resulting in a weak signal available for measurement. Based on the laser candle idea in photonics [Coffer et al., 2002], we have applied an on-resonance continuous wave excitation, modulated at the Rabi frequency ($\omega_1 = \gamma B_1$), to the Bloch equation

$$\mathbf{B}_{xy}(t) \equiv \mathbf{B}_1(t) = B_1^e(t)\cos(\omega_0 t)\mathbf{e}_x - B_1^e(t)\sin(\omega_0 t)\mathbf{e}_y, \tag{26}$$

where ω_0 is the Larmor frequency of the main static field (for simplicity we have ignored the gradient fields), and

$$B_1^e(t) = B_1\left(1 + \alpha\cos(\gamma B_1 t)\right) \tag{27}$$

in which α is a constant modulation factor, γ is the gyromagnetic ratio, and B_1 is a constant representing the amplitude of the rotating field when modulation factor is zero. After transforming the Bloch equation to the rotating frame of reference, the Rabi frequency of precession will be about the x'-direction and is given by

$$\omega_{x'}(t) = \gamma B_1[1 + \alpha\cos(\gamma B_1 t)] = \omega_1[1 + \alpha\cos(\omega_1 t)], \tag{28}$$

which clearly indicates that the Rabi frequency is time dependent. The Bloch equation for this excitation in the rotating frame of reference is

$$\dot{\mathbf{M}}'(t) = \mathbf{\Omega}'(t)\mathbf{M}'(t) + \frac{\mathbf{M}_0}{T_1}, \tag{29}$$

where

$$\mathbf{\Omega}'(t) = \begin{bmatrix} -\frac{1}{T_2} & \delta\omega & 0 \\ -\delta\omega & -\frac{1}{T_2} & \omega_1[1+\alpha\cos(\omega_1 t)] \\ 0 & -\omega_1[1+\alpha\cos(\omega_1 t)] & -\frac{1}{T_1} \end{bmatrix}, \tag{30}$$

and

$$\mathbf{M}(t=0) = \mathbf{M}_0 = \begin{bmatrix} 0 \\ 0 \\ M_0 \end{bmatrix}. \tag{31}$$

We have simulated the Bloch equation with this excitation both with and without considering field inhomogeneities. Figure 2 shows the result of four second simulation for such an excitation with $\alpha = \sqrt{3}$, and $B_1 = 100$nT. The spins system has $T_1 = 1$s, and $T_2 = 0.5$s in a 1.5T field.

The simulation results clearly shows that the magnetisation becomes very small after a period of time (in this case around 1 second) and both the transverse and longitudinal magnetisation are reborn. As can be seen after a period of time the system reaches its steady state response that is no more a constant value, but has a periodic pattern and its peak ($0.4M_0$) is comparable to the initial value which is the thermal equilibrium. The rotation frequency of the steady state response only depends on the excitation magnitude and is equal to the Rabi frequency. But the peak value of the steady state response is a function of T_1, T_2, and α.

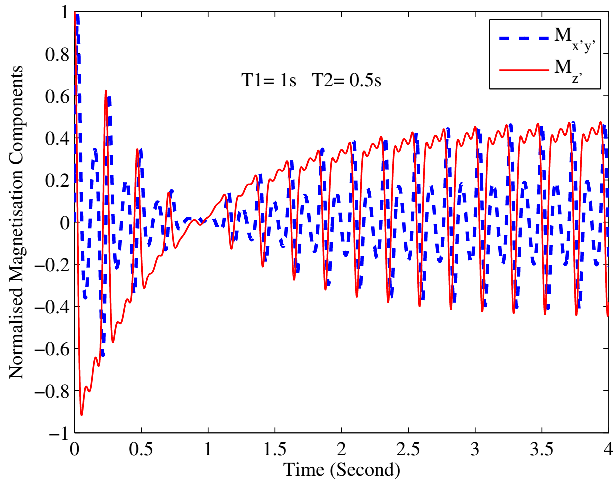

Fig. 2. Simulation result without considering field inhomogeneities under a continuous wave excitation represented by (26) with $\alpha = \sqrt{3}$, and $B_1 = 100$nT for a spin system with $T_1 = 1$s, and $T_2 = 0.5$s in a 1.5T field.

It is possible to generate signals which do not go to zero during the transient response, as shown in Figure 3. In this case, the envelope of the applied excitation pattern is

$$B_1^e(t) = B_1\left(1 + \alpha\sin(\gamma B_1 t)\right) \tag{32}$$

For comparison with the traditional MR excitation, we simulate a nonselective RF pulse for the same spin system, the results of which are shown in Figure 4. The pulse is a box-car RF field of amplitude 59μT, rotating at the Larmor frequency, for a period of 100μs. While the energy of the pulse used to generate the magnetisation shown in Figure 4 is 3.48 times of the energy of the continuous wave excitation (32), the signal intensity as measured by (18) that the continuous wave generates is twice that generated by the pulse excitation.

In the simulations to this point, we have not taken field inhomogeneities into account. Under the continuous wave excitation applied above, field inhomogeneities cause the magnetisation to die out in steady state. If, however, a stronger excitation field applied such that $\gamma B_1 >> \delta\omega$, we observe from simulations that the response of the system in the presence of field inhomogeneities becomes similar to the case without the inhomogeneities considered. It can therefore be concluded that a strong excitation field compensates for the effect of field inhomogeneities. Note that a 'strong' excitation field does not need to exceed the amplitudes generated by pulse excitation, to achieve the desired suppression of field inhomogeneities.

3.1 Periodic Solution

Since the applied modulated excitation has a periodic waveform (26), it is possible to find a periodic solution for

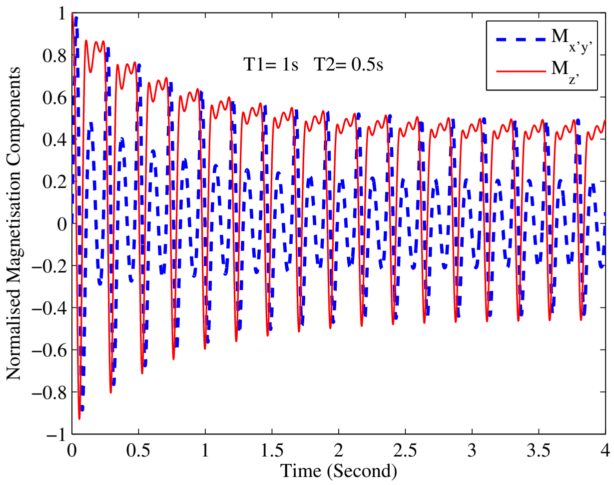

Fig. 3. Simulation result without considering field inhomogeneities under a continuous wave excitation represented by (32) with $\alpha = \sqrt{3}$, and $B_1 = 100\text{nT}$ for the same spin system in Figure 2.

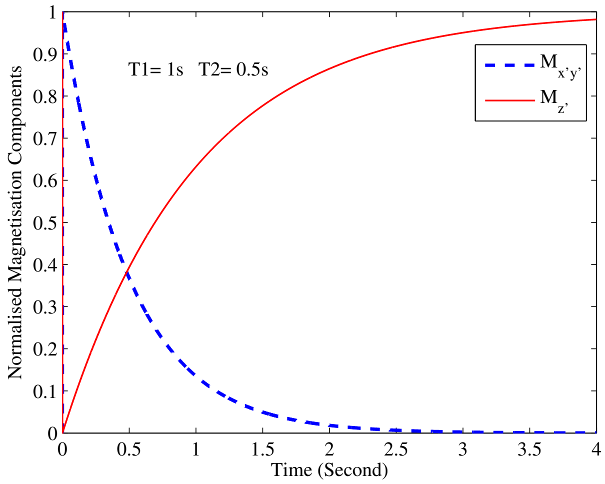

Fig. 4. Magnetisation evolution without considering field inhomogeneities under a pulse excitation for the same spin system in Figure 2.

the steady state response of the system using *Galerkin's procedure for nonlinear periodic systems* [Urabe, 1965, Donescu and Virgin, 1996]. When there are no field inhomogeneities, or alternatively when the excitation field is strong enough, $\mathbf{\Omega}'(t)$ in (29) becomes

$$\mathbf{\Omega}'(t) = \begin{bmatrix} -\frac{1}{T_2} & 0 & 0 \\ 0 & -\frac{1}{T_2} & \omega_1[1+\alpha\cos(\omega_1 t)] \\ 0 & -\omega_1[1+\alpha\cos(\omega_1 t)] & -\frac{1}{T_1} \end{bmatrix}. \tag{33}$$

It is clear that the steady state response of the x' component will be zero. Thus, we only have to find the solutions of the y', and z' components. As a result the *reduced* version of the Bloch equation may be written as

$$\dot{\mathbf{M}}'_r(t) = \mathbf{\Omega}'_r(t)\mathbf{M}'_r(t) + \frac{\mathbf{M}_{0r}(t)}{T_1}, \tag{34}$$

where

$$\dot{\mathbf{M}}'_r = \begin{bmatrix} \dot{M}_{y'} \\ \dot{M}_{z'} \end{bmatrix}, \quad \mathbf{M}'_r = \begin{bmatrix} M_{y'} \\ M_{z'} \end{bmatrix}, \quad \mathbf{M}_{0r} = \begin{bmatrix} 0 \\ M_0 \end{bmatrix}, \tag{35}$$

and

$$\mathbf{\Omega}'_r(t) = \begin{bmatrix} -\frac{1}{T_2} & \omega_1[1+\alpha\cos(\omega_1 t)] \\ -\omega_1[1+\alpha\cos(\omega_1 t)] & -\frac{1}{T_1} \end{bmatrix}. \tag{36}$$

We can rewrite $\mathbf{\Omega}'_r(t)$ as

$$\mathbf{\Omega}'_r(t) = \mathbf{A} + \mathbf{D}e^{j\omega_1 t} + \mathbf{D}e^{-j\omega_1 t}, \tag{37}$$

where

$$\mathbf{A} = \begin{bmatrix} -\frac{1}{T_2} & \omega_1 \\ -\omega_1 & -\frac{1}{T_1} \end{bmatrix}, \qquad \mathbf{D} = \begin{bmatrix} 0 & \frac{\alpha\omega_1}{2} \\ -\frac{\alpha\omega_1}{2} & 0 \end{bmatrix}. \tag{38}$$

The steady state reduced magnetisation and its derivative can be written as a summation of their harmonics,

$$\mathbf{M}'_r = \sum_{k=-\infty}^{\infty} \mathbf{C}_k e^{jk\omega_1 t}, \quad \dot{\mathbf{M}}'_r = \sum_{k=-\infty}^{\infty} jk\omega_1 \mathbf{C}_k e^{jk\omega_1 t}, \tag{39}$$

where $\mathbf{C}_k$ represents the Fourier series coefficient vector and is given by

$$\mathbf{C}_k = \left[\, C_{k_{y'}}, C_{k_{z'}} \,\right]^T. \tag{40}$$

Substituting the harmonic expansions into (34) leads to

$$\begin{aligned} \sum_{k=-\infty}^{\infty} jk\omega_1 \mathbf{C}_k e^{jk\omega_1 t} &= \mathbf{A}\sum_{k=-\infty}^{\infty} \mathbf{C}_k e^{jk\omega_1 t} + \mathbf{D}e^{j\omega_1 t}\sum_{k=-\infty}^{\infty} jk\omega_1 \mathbf{C}_k e^{jk\omega_1 t} \\ &+ \mathbf{D}e^{-j\omega_1 t}\sum_{k=-\infty}^{\infty} jk\omega_1 \mathbf{C}_k e^{jk\omega_1 t} + \frac{\mathbf{M}_{0r}}{T_1}. \end{aligned} \tag{41}$$

By balancing the harmonics and rearranging the terms,

$$\sum_{k=-\infty}^{\infty} \Big(\mathbf{A}\mathbf{C}_k - jk\omega_1 \mathbf{C}_k + \mathbf{D}\mathbf{C}_{k-1} + \mathbf{D}\mathbf{C}_{k+1} \Big) e^{jk\omega_1 t} = -\frac{\mathbf{M}_{0r}}{T_1}. \tag{42}$$

Expanding the above equation and writing it in matrix form yields $\mathbf{PC} = \mathbf{Q}$ where $\mathbf{P}$ is a block tri-diagonal matrix as follows

$$\mathbf{P} = \begin{bmatrix} \ddots & & & & \\ \mathbf{A}+j2\omega_1\mathbf{I} & \mathbf{D} & \mathbf{0} & \mathbf{0} & \mathbf{0} \\ \mathbf{D} & \mathbf{A}+j\omega_1\mathbf{I} & \mathbf{D} & \mathbf{0} & \mathbf{0} \\ \mathbf{0} & \mathbf{D} & \mathbf{A} & \mathbf{D} & \mathbf{0} \\ \mathbf{0} & \mathbf{0} & \mathbf{D} & \mathbf{A}-j\omega_1\mathbf{I} & \mathbf{D} \\ \mathbf{0} & \mathbf{0} & \mathbf{0} & \mathbf{D} & \mathbf{A}-j2\omega_1\mathbf{I} \\ & & & & \ddots \end{bmatrix}, \tag{43}$$

and

$$\mathbf{C} = \begin{bmatrix} \vdots \\ \mathbf{C}_{-2} \\ \mathbf{C}_{-1} \\ \mathbf{C}_0 \\ \mathbf{C}_1 \\ \mathbf{C}_2 \\ \vdots \end{bmatrix}, \qquad \mathbf{Q} = \begin{bmatrix} \vdots \\ \mathbf{0} \\ \mathbf{0} \\ -\dfrac{\mathbf{M}_{0r}}{T_1} \\ \mathbf{0} \\ \mathbf{0} \\ \vdots \end{bmatrix}. \tag{44}$$

Through inversion of $\mathbf{P}$ it is possible to calculate the coefficients of the Fourier series. $\mathbf{P}$ is an infinite matrix however, and to approximate the coefficients this matrix must be truncated. The convergence rate of the coefficients must be found, to ensure a desired accuracy is achieved when truncating the series solution. By decomposing $\mathbf{P}$ into a product of lower and upper triangular matrices, we have proven that the convergence rate of the periodic solution is $(\frac{\alpha}{2})^N/N!$, where N indicates the order of truncation [Tahayori et al., 2007]. The Fourier series coefficients therefore converge to zero at a surprisingly fast rate. Simulation results support this analytic convergence rate. When the modulation factor (see (27)) $\alpha \leq 2$, five terms are enough to ensure less than 1% relative error.

4. CONCLUSION

In this paper we have formulated the problem of designing the optimal excitation pattern for Magnetic Resonance Imaging based on a Signal Contrast Efficiency performance measure. An excitation pattern was represented that maintains the coherency of the spins in the steady state. Moreover, it was shown that this continuous wave excitation can generate an improved signal intensity for a single tissue type, relative to the traditional pulse excitation.

It is important to note that obtaining a better MR Signal Contrast Efficiency, through design of a better excitation pattern, does not necessarily lead to a superior image; localisation of the signal plays a key role in image formation. Nonetheless, it is always possible to make an image from the received MR signal, for example using the backprojection technique [Prince, 1996], regardless of the excitation waveform. There is no guarantee that this method of image reconstruction is as efficient as the Fourier method. However the first step towards the generation of MR images with higher quality is the acquisition of the optimal system response to input excitation of a given amount of energy. Signal localisation forms the second step in the procedure. Eventually both aspects of the problem must be taken into consideration, however we advocate solution of the optimisation in two separate steps, given the difficult nature of formulating and then solving the problem that fuses the both steps.

If in future work it is found that the answer to the MR excitation problem, as posed in this paper, is pulse excitation, then we will have provided a proof of optimality of the pulse excitation, and the result may be used to design better pulse sequences. If, on the other hand, the solution to the problem is a class of waveforms other than pulse excitation, then horizons in MRI research will have been broadened, with the potential to affect all forms of MR imaging, including structural MRI, functional MRI (fMRI), Diffusion Tensor Imaging (DTI), perfusion imaging, and Magnetic Resonance Angiography (MRA).

REFERENCES

A.D. Alster and J.H. Burdette. *Questions and Answers in Magnetic Resonance Imaging*. Mosby, 2nd edition, 2001.

R. Brockett and N. Khaneja. Optimal input design for NMR system identification. *Proceedings of the 40th Conference on Decesion and Control*, pages 4128–4133, 2001.

J.G. Coffer, B. Sickmiller, A. Presser, and J.C. Camparo. Line shapes of atomic-candle-type Rabi resonances. *Physical Review*, 66:0238061–0238067, 2002.

S. Conolly and A. Macovski. Selective excitation via optimal control theory. *Proceedings of the 4th Meeting of the Society of Magnetic Resonance in Medicine*, page 958, 1985.

S. Conolly, D. Nishimura, and A. Macovski. Optimal control solutions to the magnetic resonance selective excitation. *IEEE Transactions on Medical Imaging*, 5: 106–115, 1996.

P. Donescu and L.N. Virgin. Efficient determination of higher-order periodic solutions using n-mode harmonic balance. *IMA Journal of Applied Mathematics*, 56:21–32, 1996.

A. Garroway, P. Grannell, and P. Mansfield. Image formation in NMR by a selective irradiative process. *Journal of Physics*, 7:457–462, 1974.

E.M. Haacke, R.W. Brown, M.R. Thompson, and R. Venkatsen. *Magnetic Resonance Imaging, Physical Principles and Sequence Design*. Wiley-Liss, 1999.

W.S. Hinshaw and A.H. Lent. An introduction to NMR imaging, from the Bloch equation to the imaging equation. *Proceedings of the IEEE*, 71:338–350, 1983.

M.H. Levitt. *Spin Dynamics, Basics of Nuclear Magnetic Resonance*. Wiley, 2001.

Jr-Shin Li and Navin Khaneja. Control of inhomogeneous quantum ensembles. *Physical Review A*, 73:030302, 2006.

W. Loeffler, A. Opplet, and D. Faul. Computer simulations of slice selection in NMR imaging. *Proceedings of the 2nd Meeting of the Society of Magnetic Resonance in Medicine*, pages 196–197, 1983.

J. Pauly, P. Le Roux, D. Nishimura, and A. Macovski. Parameter relations for the Shinnar-Le Roux selective excitation pulse design algorithm. *IEEE Transactions on Medical Imaging*, 10:33–65, 1991.

J.L. Prince. Convolution backprojection formulas for 3-d vector tomography with application to MRI. *IEEE Transactions on Image Processing*, 5:1462–1472, 1996.

B. Tahayori, L.A. Johnston, I.M.Y. Mareels, and P.M. Farrell. Optimisation of the magnetic resonance signal. Technical Report TR07-010, University of Melbourne, 2007.

J.L. Ulloa, M. Guarini, A. Guesalaga, and P. Irarrazaval. Chebyshev series for designing RF pulses employing an optimal control approach. *IEEE Transactions on Medical Imaging*, 23:1445–1452, 2004.

M. Urabe. Galerkin's procedure for nonlinear periodic systems. *Archive for Rational Mechanics and Analysis*, 20:120–152, 1965.